A radio-frequency sheath model for complex waveforms

M. M. Turner and P. Chabert

Citation: Applied Physics Letters **104**, 164102 (2014); doi: 10.1063/1.4872172
View online: http://dx.doi.org/10.1063/1.4872172
View Table of Contents: http://scitation.aip.org/content/aip/journal/apl/104/16?ver=pdfcov
Published by the AIP Publishing

A radio-frequency sheath model for complex waveforms

M. M. Turner[1] and P. Chabert[2]
[1]*School of Physical Sciences and National Centre for Plasma Science and Technology, Dublin City University, Dublin 9, Ireland*
[2]*Laboratoire de Physique des Plasmas, Centre National de la Recherche Scientifique, Ecole Polytechnique, Université Pierre et Marie Curie, Paris XI, 91128 Palaiseau, France*

(Received 28 July 2013; accepted 10 April 2014; published online 21 April 2014)

Plasma sheaths driven by radio-frequency voltages occur in contexts ranging from plasma processing to magnetically confined fusion experiments. An analytical understanding of such sheaths is therefore important, both intrinsically and as an element in more elaborate theoretical structures. Radio-frequency sheaths are commonly excited by highly anharmonic waveforms, but no analytical model exists for this general case. We present a mathematically simple sheath model that is in good agreement with earlier models for single frequency excitation, yet can be solved for arbitrary excitation waveforms. As examples, we discuss dual-frequency and pulse-like waveforms. The model employs the ansatz that the time-averaged electron density is a constant fraction of the ion density. In the cases we discuss, the error introduced by this approximation is small, and in general it can be quantified through an internal consistency condition of the model. This simple and accurate model is likely to have wide application. © *2014 AIP Publishing LLC*. [http://dx.doi.org/10.1063/1.4872172]

In many radio-frequency discharges, the sheath is the most important region, because impedance, power absorption, and ion acceleration are dominated by sheath processes.[1,2] There are other contexts where radio-frequency sheath physics is a concern, for example, when understanding the physics of heating in both fusion plasmas[3–5] and discharges.[6,7] Consequently, models of the sheath are important, either in themselves or as elements in more complex situations, over a broad area of plasma physics. The problem has been considered on a number of occasions, e.g., Refs. 8–11. Analytical models are particularly useful for developing physical insight and expressing the relationships between parameters in a clear way, but such models have proved elusive. Lieberman[1,12] supplied an analytical model for a radio-frequency sheath driven by a single frequency, but in practice much more complex waveforms frequently occur.[13–17] There has been limited success in generalizing the Lieberman's model to cover these cases because of intractable mathematical complexities.[18–20] So there is essentially no sheath model available to describe many modern experiments. This paper presents an analytical sheath model that simplifies Lieberman's[1,12] model using one additional ansatz that we discuss below. As we shall show, this ansatz has no practical effect on the accuracy of the model, but permits essentially arbitrary excitation waveforms to be treated. For the single frequency case, however, the present model yields scaling laws that are identical in form to those of Lieberman's model,[1,12] differing only by numerical coefficients close to one.

A sheath in the radio-frequency regime, shown schematically in Fig. 1, is characterised by a time-varying electron density, $n_e(x,t)$, and a stationary ion density, $n_i(x)$, which is determined by the time-averaged electrostatic potential, $\bar{\phi}(x)$. The latter is found by solving Poisson's equation, with the time-averaged sheath voltage $\bar{V}$ as a boundary condition and with the time-averaged electron density, $\bar{n}_e$ included in the source term. An important parameter in this context is

$$\xi = \frac{\bar{V}}{V_0}, \tag{1}$$

where V_0 is the maximum sheath voltage. There are no electrons in the sheath when the sheath voltage is a maximum. One can quickly show that for a sheath of width s_m, consistency between $\bar{\phi}(x)$ and the potential at maximum sheath voltage requires

$$\int_0^{s_m} dx' \int_0^{x'} dx''[(1-\xi)n_i - \bar{n}_e] = 0, \tag{2}$$

which is satisfied (but not uniquely) by the choice $\bar{n}_e = (1-\xi)n_i$, which is our ansatz. The difference between the Lieberman's sheath model[12] and the Child-Langmuir's model[21] arises mostly from the presence of electron space charge in the sheath. In combination with other constraints of the model, our ansatz introduces an appropriate amount of electron space-charge, but approximates the spatial distribution of this charge. Thus, the time-averaged charge density is $\bar{\rho} = e\xi n_i$. Hence, we can write down the transport equations for ions of mass M and drift velocity $u_i(x)$

$$n_i u_i = n_0 u_B, \tag{3}$$

$$e\bar{\phi} + \frac{1}{2}Mu_i^2 = \frac{1}{2}Mu_B^2 \approx 0, \tag{4}$$

$$\frac{d^2\bar{\phi}}{dx^2} = -\frac{e\xi n_i}{\epsilon_0}, \tag{5}$$

where a constant ion current $J_i = en_0u_B$ enters the sheath at $x=0$, $u_B = \sqrt{k_BT_0/M}$, n_0 and T_0 are the density and electron temperature of a quasi-neutral plasma filling the space $x<0$,

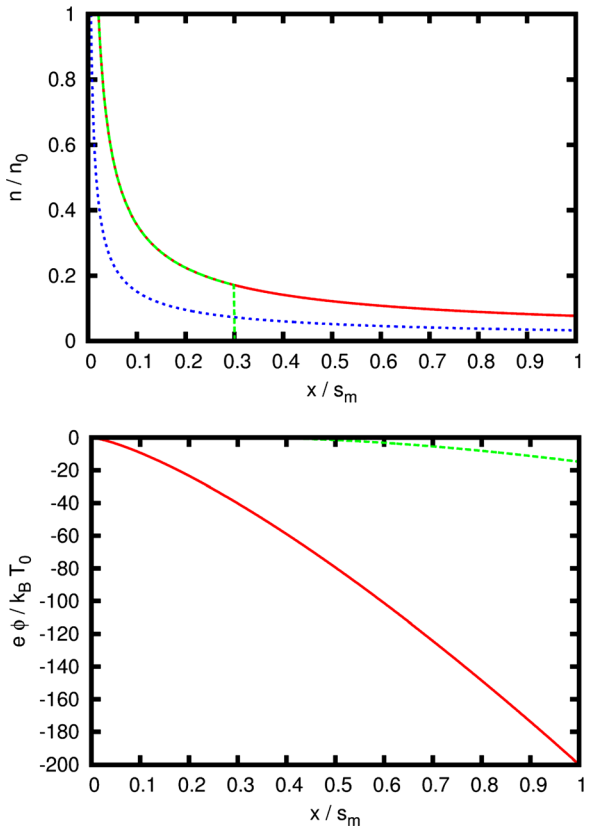

FIG. 1. Upper panel: Charged particle densities, showing the ion density, n_i (solid line); the time averaged electron density, $\bar{n}_e$ (dotted line); and the electron density, n_e at the instant when $s/s_m = 0.3$ (dashed line). Lower panel: Electrostatic potential, showing the time averaged potential, $\bar{\phi}$ (solid line) and the instantaneous potential when $s/s_m = 0.3$ (dashed line).

and we assume $e\bar{V} \gg k_B T_0$. These equations are those of the Child-Langmuir sheath model,[1,2,21,22] with the addition of the parameter ξ, and we can at once write down the solutions

$$J_i = K_i \frac{\epsilon_0}{s_m^2}\left(\frac{2e}{M}\right)^{\frac{1}{2}}(-\bar{V})^{\frac{3}{2}}, \tag{6}$$

$$n_i(x) = -\frac{4}{9}\frac{\epsilon_0 \bar{V}}{\xi e s_m^2}\left(\frac{s_m}{x}\right)^{\frac{2}{3}}, \tag{7}$$

$$\bar{\phi}(x) = \bar{V}\left(\frac{x}{s_m}\right)^{\frac{4}{3}}, \tag{8}$$

where the electric field vanishes at $x = 0$ and where $K_i = 4/(9\xi)$. The time-dependent field and potential can now be determined by integrating Poisson's equation again, with the approximation[11,12] that

$$n_e(x,t) = \begin{cases} 0 & \text{if } s(t) < x \le s_m \\ n_i(x) & \text{otherwise,} \end{cases} \tag{9}$$

where $s(t)$ is the position of the sheath edge, at which point the electric field and the potential vanish. This procedure gives the time dependent sheath voltage $V(t)$, potential $\phi(x,t)$, and electric field $E(x,t)$. Now

$$J(t) = \epsilon_0 \frac{\partial E}{\partial t}\bigg|_{x=s_m} = \frac{4}{3}\frac{\epsilon_0 V_0}{s_m}\frac{d}{dt}\left(\frac{s(t)}{s_m}\right)^{\frac{1}{3}}. \tag{10}$$

Adopting the convention $J(t=0) = 0$, we find

$$\frac{s(t)}{s_m} = \left[\frac{3}{4}\frac{s_m}{\epsilon_0 V_0}\int_0^t J dt\right]^3. \tag{11}$$

Since $0 \le s/s_m \le 1$, once $J(t)$ is chosen, $s(t)/s_m$ is fully defined and we can express

$$\xi = \frac{\langle V(t)\rangle}{V_0} = \left\langle 1 - \frac{4}{3}\left(\frac{s(t)}{s_m}\right)^{\frac{1}{3}} + \frac{1}{3}\left(\frac{s(t)}{s_m}\right)^{\frac{4}{3}}\right\rangle. \tag{12}$$

Hence, once $J(t)$ has been given, all the remaining quantities can be calculated without further assumption or approximation, as shown in the examples below. A consequence of our ansatz is that the solution of Eq. (2) is not consistent with Eq. (9). For an excitation waveform with period T

$$\bar{n}_e \equiv \xi n_i \neq \frac{1}{T}\int_0^T n_e(x,t)dt, \tag{13}$$

when $n_e(x,t)$ is given by Eq. (9). In Lieberman's model, there is strict equality here. Thus, this is an internal consistency condition of the present model that can be used to quantify the error introduced by the ansatz. This error can be shown to be small in the cases we discuss below.

For the single frequency case treated by Lieberman,[12] we choose $J(t) = -J_0 \sin \omega t$. From Eqs. (11) and (12), we find

$$s(t) = \frac{s_m}{8}(1 - \cos \omega t)^3, \tag{14}$$

$$J_0 = -\frac{K_{\text{cap}}}{2}\frac{\omega \epsilon_0}{s_m} V_0, \tag{15}$$

$$\xi = \frac{163}{384}, \tag{16}$$

$$s_m = \frac{K_s J_0^3}{e\epsilon_0 k_B T_0 \omega^3 n_0^2}, \tag{17}$$

where $K_{\text{cap}} = 4/3$ and $K_s = 4\xi/3$. These expressions are identical with those of Lieberman,[1,12] apart from numerical coefficients close to unity, as shown in Table I. A metric for the quality of our approximation is the inequality in Eq. (13), which is ~10% in all the examples we discuss. This error is small because the boundary conditions closely constrain the line integrals of both the positive and negative space charge components, and the smoothing qualities of the Laplacian operator render the potential and the field insensitive functions of the spatial distribution of this charge. The present

TABLE I. Comparison of numerical coefficients in Eqs. (17), (15), and (6) determined from three different models.

	Present	Lieberman
ξ	0.425	0.415
K_{cap}	1.33	1.23
K_i	1.05	0.82
K_s	0.566	0.417

model is therefore not appreciably inferior in accuracy to that of Lieberman, but can be solved for a far greater range of waveforms. In particular, the current density can be expressed as an arbitrary Fourier series, leading, for example, to models for multiple-frequency excitation that are free of inconvenient restrictions on the component amplitudes (such as occur in dual-frequency generalizations of Lieberman's model[18–20]).

For example, we can choose

$$J(t) = -J_0 \sin \omega_0 t - J_1 \sin \omega_1 t \tag{18}$$

and find at once

$$s(t) = \frac{s_m}{8}\left[\frac{(J_0/\omega_0)(1-\cos\omega_0 t) + (J_1/\omega_1)(1-\cos\omega_1 t)}{J_0/\omega_0 + J_1/\omega_1}\right]^3, \tag{19}$$

$$J_0 = -\frac{2}{3}\frac{\omega_0 \epsilon_0 V_0}{s_m}\left(1 + \frac{J_1\omega_0}{J_0\omega_1}\right), \tag{20}$$

$$s_m = \frac{4\xi}{3}\frac{(J_0/\omega_0 + J_1/\omega_1)^3}{\epsilon_0 e n_0^2 k_B T_0}, \tag{21}$$

$$\xi = \frac{1}{3} + \frac{\frac{35}{128}\left[\left(\frac{J_0}{\omega_0}\right)^4 + \left(\frac{J_1}{\omega_1}\right)^4\right] + \frac{5}{8}\left[\left(\frac{J_0}{\omega_0}\right)^3\frac{J_1}{\omega_1} + \frac{J_0}{\omega_0}\left(\frac{J_1}{\omega_1}\right)^3\right] + \frac{27}{32}\left(\frac{J_0}{\omega_0}\right)^2\left(\frac{J_1}{\omega_1}\right)^2}{(J_0/\omega_0 + J_1/\omega_1)^4}, \tag{22}$$

$$\approx \frac{163}{384}, \tag{23}$$

where we note that Eq. (22) yields a result never different by more than 10% from the single frequency result, which value can therefore be used for all practical purposes. These formulae are therefore more generally applicable, less cumbersome, and obtained with less mathematical exertion than those previously given.[18–20]

As a third example, we consider a sheath excited by the pulsed waveform

$$J(t) = J_0\left(\frac{t}{t_w}\right)\exp\left(\frac{1}{2} - \frac{1}{2}\frac{t^2}{t_w^2}\right), \tag{24}$$

which is representative of several topical experiments.[13–15] We assume that this pulse is repeated at intervals $t_p \ll t_w$, such that successive pulses do not appreciably overlap. In this case, we find

$$s(t) = s_m \exp\left(-\frac{3}{2}\frac{t^2}{t_w^2}\right), \tag{25}$$

$$\xi = 1 - \frac{7}{3}\sqrt{\frac{\pi}{2}}\frac{t_w}{t_p}, \tag{26}$$

$$J_0 = -\frac{4}{3}\frac{\epsilon_0 V_0}{s_m t_w \exp\left(\frac{1}{2}\right)}, \tag{27}$$

$$s_m = \frac{\xi}{6}\exp\left(\frac{3}{2}\right)\frac{(J_0 t_w)^3}{\epsilon_0 e n_0^2 k_B T_0}. \tag{28}$$

The Child law and therefore the sheath width are found by inserting Eq. (26) into Eq. (6). We have investigated the utility of this model by comparison with particle-in-cell simulation data.[23,24] These simulations treated a plasma formed in a space between two plane parallel electrodes separated by 6.7 cm, filled with argon gas at a pressure of 10 mTorr or 1.33 Pa, and excited by a current density with the form of Eq. (24). Relevant electron and ion collisional processes are included, but secondary emission phenomena are not. The peak current density ranged from 5 to 70 A m^{-2} and the pulse width ranged from approximately 1 to 10 ns. These conditions lead to $T_0 \approx 1.5$ eV and $n_0 \approx 3\times10^{14} - 3\times10^{15}$ m^{-3}. In Figs. 2–4, we compare these simulation results with the predictions of the present model, and we find good agreement both for time dependent currents and voltages and scaling laws. These figures collapse rather complicated scans over two parameters (J_0 and τ_w) onto single curves.

To summarize, in this paper, we have developed a sheath model that can be expressed in a small number of straightforward equations. We have also shown how to quantify the error in this model. For the single-frequency case, the model agrees well with the Lieberman's model. The

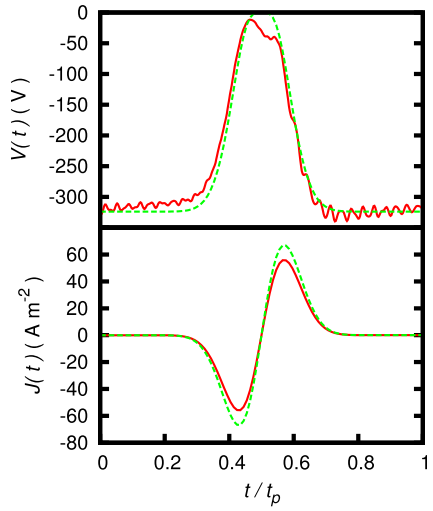

FIG. 2. Comparison of simulation results (solid lines) with the analytical theory of the text (dashed lines) for sheath voltage (upper panel) and sheath current density (lower panel). For this case, $t_w = 5.2$ ns. The electrical control parameter for the sheath model is $\bar{V}$, the time averaged sheath voltage, which is here chosen to be the same as in the simulation.

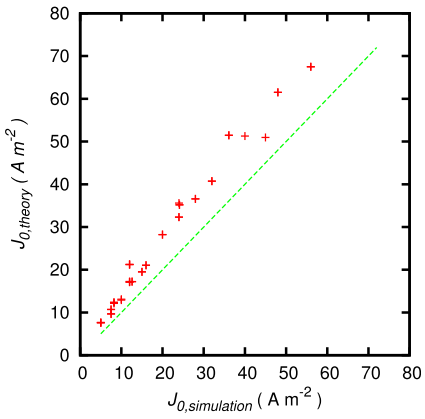

FIG. 3. Comparison of the maximum radio-frequency current density found in simulation (horizontal axis) with the result computed from Eq. (27) (vertical axis). The solid line denotes ideal agreement between theory and simulation.

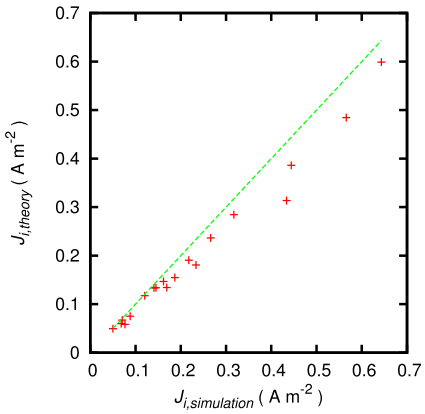

FIG. 4. Comparison of the ion current density found in simulation (horizontal axis) with the result computed from Eqs. (6) and (26) (vertical axis). The solid line denotes ideal agreement between theory and simulation.

Lieberman's model, in spite of its elegant construction, is mathematically complex and has proved resistant to generalization. The present model, however, is readily adaptable to a wide range of complex excitation waveforms and leads to results in good agreement with simulations. Thus, this model provides a valuable tool for designing and understanding experiments involving non-sinusoidal excitation of radio-frequency sheaths.

The work of M.M.T. was supported by Science Foundation Ireland under Grant Nos. 07/IN.1/I907 and 08/SRC/I1411. The work of P.C. was supported by the Agence Nationale de le Recherche (CANASTA Project No. ANR-10-HABISOL-002).

[1]M. A. Lieberman and A. J. Lichtenberg, *Principles Of Plasma Discharges and Materials Processing* (John Wiley & Sons, 2005).
[2]P. Chabert and N. S. J. Braithwaite, *Physics of Radio-Frequency Plasmas* (Cambridge University Press, 2011).
[3]D. A. D'Ippolito, J. R. Myra, J. Jacquinot, and M. Bures, Phys. Fluids B **5**, 3603 (1993).
[4]L. Colas, A. Ekedahl, M. Goniche, J. P. Gunn, B. Nold, Y. Corre, V. Bobkov, R. Dux, F. Braun, J.-M. Noterdaeme *et al.*, Plasma Phys. Controlled Fusion **49**, B35 (2007).
[5]J. R. Myra and D. A. D'Ippolito, Phys. Rev. Lett. **101**, 195004 (2008).
[6]P. Chabert, J. L. Raimbault, P. Levif, J. M. Rax, and M. A. Lieberman, Phys. Rev. Lett. **95**, 205001 (2005).
[7]M. M. Turner and P. Chabert, Phys. Rev. Lett. **96**, 205001 (2006).
[8]F. Schneider, Z. Angew. Phys. **6**, 456 (1954).
[9]H. S. Butler and G. S. Kino, Phys. Fluids **6**, 1346 (1963).
[10]V. A. Godyak, *Soviet Radio Frequency Discharge Research* (Delphic Associates, 1986).
[11]R. P. Brinkmann, J. Phys. D: Appl. Phys. **42**, 194009 (2009).
[12]M. Lieberman, IEEE Trans. Plasma Sci. **16**, 638 (1988).
[13]S.-B. Wang and A. E. Wendt, J. Appl. Phys. **88**, 643 (2000).
[14]B. G. Heil, U. Czarnetzki, R. P. Brinkmann, and T. Mussenbrock, J. Phys. D: Appl. Phys. **41**, 165202 (2008).
[15]E. V. Johnson, T. Verbeke, J.-C. Vanel, and J.-P. Booth, J. Phys. D: Appl. Phys. **43**, 412001 (2010).
[16]E. V. Johnson, P. A. Delattre, and J. P. Booth, Appl. Phys. Lett. **100**, 133504 (2012).
[17]T. Lafleur, R. W. Boswell, and J. P. Booth, Appl. Phys. Lett. **100**, 194101 (2012).
[18]J. Robiche, P. C. Boyle, M. M. Turner, and A. R. Ellingboe, J. Phys. D: Appl. Phys. **36**, 1810 (2003).
[19]R. N. Franklin, J. Phys. D: Appl. Phys. **36**, 2660 (2003).
[20]P. C. Boyle, J. Robiche, and M. M. Turner, J. Phys. D: Appl. Phys. **37**, 1451 (2004).
[21]C. D. Child, Phys. Rev. (Ser. I) **32**, 492 (1911).
[22]I. Langmuir, Phys. Rev. **2**, 329 (1913).
[23]C. K. Birdsall and A. B. Langdon, *Plasma Physics via Computer Simulation* (Adam Hilger, 1991).
[24]C. K. Birdsall, IEEE Trans. Plasma Sci. **19**, 65 (1991).